Predictive Thermodynamic Modeling of Poorly Specified Mixtures and Applications in Conceptual Fluid Separation Process Design

Thomas Specht, Hans Hasse, and Fabian Jirasek*

Laboratory of Engineering Thermodynamics (LTD), RPTU Kaiserslautern, Erwin-Schrödinger-Straße 44, 67663 Kaiserslautern, Germany

E-mail: *fabian.jirasek@rptu.de

Abstract

In many chemical engineering processes, mixtures occur whose composition is not well known. Simulations of processes with such poorly specified mixtures are basically unfeasible, as thermodynamic models require knowledge of the speciation. As a workaround, pseudo-components can be introduced, which are generally defined using ad-hoc assumptions. In a previous series of works, we have developed and tested a method for quantifying the group composition of poorly specified mixtures based on simple NMR experiments, without having to solve the much more complicated task of quantifying all species. This method has been extended recently to a rational method for defining pseudo-components in poorly specified mixtures. In the present work, this method is combined with several thermodynamic group-contribution methods. The resulting thermodynamic models were applied to various poorly specified mixtures and used for solving two typical tasks from conceptual fluid separation process design: a) solvent screening for liquid-liquid extraction processes and b) simulation of open evaporation processes. The results show excellent agreement with those obtained using the

complete information on the speciation, which was known for the studied test mixtures but disregarded in applying the new approach.

Introduction

Modeling and simulation are essential for process development and optimization. In the present work, we focus on fluid separation processes, namely liquid-liquid extraction and distillation. For modeling such processes, information on the phase equilibria is needed, which is typically supplied in the form of models of the Gibbs excess energy G^{E}, such as NRTL,[1] UNIQUAC,[2] or the group-contribution method UNIFAC.[3,4] These models, as well as all other thermodynamic models, require a complete specification of the composition of the studied mixture. However, there are many applications in which information on the composition is lacking, e.g., in petroleum engineering,[5,6] bioprocess engineering,[7] and wastewater treatment.[8]

A common approach to circumvent this problem is the introduction of pseudo-components, which can be done in a discrete manner[9–11] or using continuous thermodynamics.[12–15] However, in both cases, the definition of pseudo-components is usually based on ad-hoc assumptions regarding the nature and number of pseudo-components. Moreover, such pseudo-component methods are typically tailored for the description of a specific class of mixtures - and they often require carrying out tailored experiments as a basis for the modeling, such as measurements of the so-called true boiling point curve of crude oil, which is used in petroleum engineering for defining pseudo-components by introducing a certain number of temperature cuts.[16,17]

We have recently introduced a new generic way to define and quantify pseudo-components that is free from ad-hoc assumptions.[18] It is based on a series of previous papers, in which we have introduced a method for quantifying the group composition of poorly specified mixtures based on simple NMR experiments.[19–23]

Nuclear magnetic resonance (NMR) spectroscopy is a non-invasive analytical technique frequently used for elucidating and quantifying components in mixtures.[24–29] However, for complex mixtures, the complete elucidation and quantification of the components may be practically infeasible. The task is much easier if only structural groups are identified and quantified instead of the components. The basis for identifying structural groups from NMR spectra is that the position of a peak in an NMR spectrum, the so-called chemical shift, directly depends on the environment of the respective nucleus, i.e., the structural group to which the nucleus that gives rise to the peak belongs.[30]

In our first works,[19–23] the quantification of the group composition was carried out using standard ^{1}H or ^{13}C NMR experiments. Using additionally ^{13}C distortionless enhancement by polarisation transfer (DEPT) NMR experiments,[30] as done in subsequent work,[18] is beneficial, as this enables reliable discrimination of the substitution degree of the carbon atoms, which is valuable information for group-contribution methods. The NMR method that yields the group composition of a poorly specified mixture is designated as *NMR fingerprinting* in the following.

The sole NMR fingerprinting was recently extended to a method for defining and quantifying pseudo-components in poorly specified mixtures.[18] For this purpose, in addition to the NMR fingerprinting, also ^{13}C pulsed-field gradient (PFG) NMR experiments[31–33] were carried out, which enable assigning self-diffusion coefficients to structural groups. The results are usually displayed in a so-called diffusion-ordered spectroscopy (DOSY) map, where the chemical shifts of the groups are displayed over their self-diffusion coefficients. As groups on the same molecule have the same self-diffusion coefficient, this technique can reasonably cluster the identified groups into pseudo-components. These pseudo-components may be identical to actual components, but groups of different components with similar diffusion coefficients may also be clustered into the same pseudo-component. A K-medians algorithm was used for the clustering, and the optimal number of clusters (pseudo-components) K was found from maximizing the silhouette score.[18,34]

With the procedure so far described, the *ratio* of the different groups in all K pseudo-components can be determined - but not the *absolute* numbers of groups in each pseudo-component. However, the information on the self-diffusion coefficient of the pseudo-components from the PFG NMR experiments can also be used to determine the molar mass of the pseudo-components and, thereby, the absolute numbers of groups in the components. Such a procedure is possible since a component's diffusion coefficient and molar mass are closely related. This relation is encoded in all methods for estimating diffusion coefficients, which typically consider the diffusion coefficient of a solute at infinite dilution, which is identical to the self-diffusion coefficient of the solute. In Ref.,[18] the Stokes–Einstein Gierer-Wirtz estimation (SEGWE) model[35,36] was used to estimate the molar masses from the self-diffusion coefficients of the pseudo-components. In a recent study, it was found that the SEGWE model is the best semi-empirical model for predicting self-diffusion coefficients.[37]

These steps finally result in a quantitative representation of the unknown components in a mixture by K pseudo-components $\tilde{\mathrm{U}}_k$, described by their structural group composition. The obtained numbers for the structural groups of type g in pseudo-component k, denoted by $\nu_{g,k}$, may have non-integer values as several true components with different concentrations can be lumped into a single pseudo-component. However, this does not hinder the application of the results for predicting many thermodynamic properties, such as normal-boiling points,[38] vapor pressures,[39] critical properties,[40] or even quantum-chemical descriptors[41] and activity coefficients[3,42] using respective group-contribution methods. Hence, this procedure allows the prediction of thermodynamic properties of mixtures without the need to elucidate the unknown components' molecular structure. Such modeling generally requires mapping the group distribution scheme used in defining the pseudo-components to that used in the thermodynamic group-contribution method, which is a task that usually can be solved.

In summary, the quantitative analysis of group compositions via NMR fingerprinting together with a rational approach for defining pseudo-components yields, in principle, all pieces of information that are required for modeling processes with poorly specified mixtures

– without the need to elucidate and quantify all true species, which can become highly elaborate in practice.

In the present work, we demonstrate the applicability of this approach for predictive thermodynamic modeling of poorly specified mixtures - and the usefulness of the resulting models for fluid separation process design.[43] For this purpose, the phase behavior of various poorly specified mixtures was predicted. The results were used for solvent screening for liquid-liquid extraction processes and for simulating open evaporation processes by predicting residue curves. All this is done without knowing the exact composition of the mixture. The group-contribution method UNIFAC[3,4] was used to predict the activity coefficients for the phase equilibrium calculations. Furthermore, a method for the description of the vapor pressure[38,39] of the pseudo-components, which is needed for the description of vapor-liquid equilibria, was employed. Note that although only liquid-liquid equilibria and vapor-liquid equilibria are considered in this work, the methodology can also be extended to other types of phase equilibria, like solid-liquid equilibria or vapor-liquid-liquid equilibria, straightforwardly; the only prerequisite for doing so is that suitable group-contribution methods for the respective relevant fluid properties are available.

Methods

Overview of the Workflow

Figure 1 summarizes all steps of the procedure applied in the present work. The methodology for NMR fingerprinting and the pseudo-component method, cf. upper part of Figure 1, were adopted from prior work;[18] the main contribution of this work is the application of the respective results together with thermodynamic group-contribution methods for predicting phase equilibria and simulating thermal separation processes, cf. lower part of Figure 1.

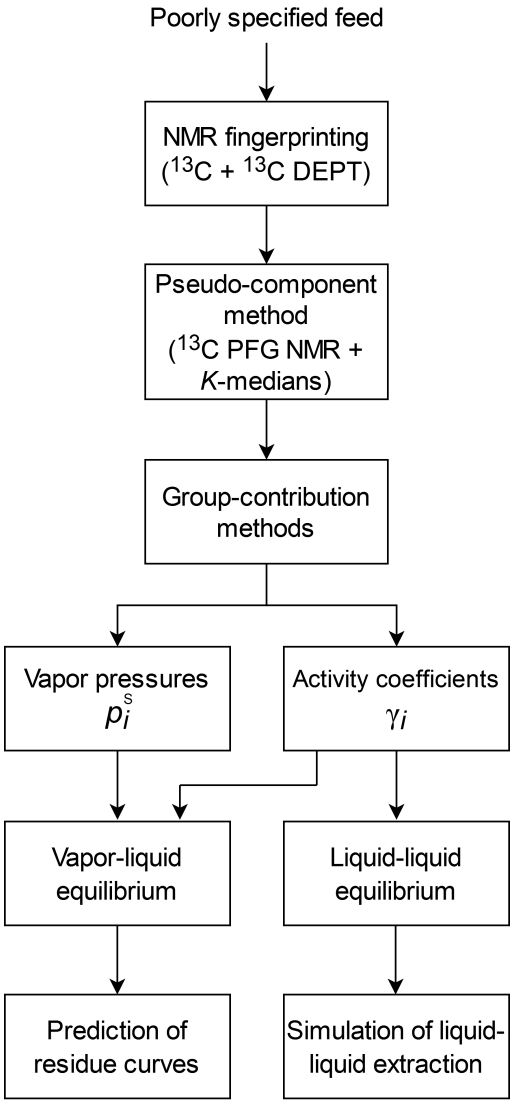

Figure 1: Schematic overview of the workflow applied in the present work. The NMR fingerprinting method and the pseudo-component method were adopted from prior work.[18] Their results were used to simulate liquid-liquid extraction processes and predict residue curves for open evaporation processes with poorly specified feeds.

NMR Fingerprinting and Pseudo-Component Method

No experiments were carried out in the present work. The NMR-spectroscopic information of the studied mixtures required for the NMR fingerprinting, namely the ^{13}C NMR and ^{13}C DEPT NMR spectra, was taken from previous work.[18]

The NMR fingerprinting was based on the approach of our previous work,[18] in which the groups identified in the fingerprinting were already mapped to groups of UNIFAC.[3,4] Additionally, in this work, also a mapping of the groups determined in the fingerprinting to the groups of the method of Refs.[38,39] for the prediction of vapor pressures was carried out. For technical details, we refer to the Supporting Information.

Table 1 summarizes the structural groups distinguished in this work together with the mapping to the groups of UNIFAC[3,4] and the method of Refs.[38,39] Furthermore, Table 1 also indicates the assignment of each group to regions of chemical shift, taking into account the substitution degree of the carbon atoms, which was obtained by considering ^{13}C DEPT NMR spectra.

Table 1: Mapping of groups identified and quantified by NMR fingerprinting based on ^{13}C and ^{13}C DEPT NMR to those from Refs.[38,39] and UNIFAC.[3,4,44] Carbon atom classification: P primary, S secondary, T tertiary, Q quaternary). The numbers in parentheses correspond to the group identifiers in the publications of the original methods.[3,4,38,39,44]

^{13}C NMR chemical shift region	Carbon	Nannoolal[38,39] label	UNIFAC[3,4,44] label
0-60 ppm	P	CH3 (1)	CH3 (1)
	S	CH2 (4)	CH2 (2)
	T	CH (5)	CH (3)
	Q	C (6)	C (4)
60-90 ppm	S	CH2 (7) + OH(P) (35/36)[a]	CH2 (2) + OH (14)
	T	CH (7) + OH(S) (34)	CH (3) + OH (14)
	Q	C (7) + OH(T) (33)	C (4) + OH (14)
90-150 ppm	S/T	CH=CH (58)	CH=CH (6)
	Q	C=C (58)	C=C (70)
150-180 ppm	Q	COOH (44)	COOH (42)
>180 ppm	T	CHO (52)	CHO (20)
	Q	CO (51)	CH3CO (18) / CH2CO (19)

[a] If the number of carbon atoms in the pseudo-component is less than five, group 36 was used, otherwise group 35 was used, as recommended in Refs.[38,39]

The quantification of the groups was done by a manual integration of the respective peaks in the quantitative ^{13}C NMR spectrum, as described in our prior work.[18]

The method used for the quantitative definition of pseudo-components based on the NMR fingerprinting and the diffusion coefficients measured by ^{13}C PFG NMR experiments was also adopted from prior work.[18] From this, the composition of each poorly specified mixture was obtained, cf. Supporting Information for details. Three mixtures were considered in the present work as examples (details are given below). Their composition was known from gravimetric preparation, but that information was not used in the study except for a comparison of the results. Hence, we label them as poorly specified mixtures in the following.

Simulation of Liquid-liquid Extraction Processes

The studied poorly specified mixtures were considered as feeds of a single-stage liquid-liquid extraction described with an equilibrium-stage model. The task was to compare the per-

formance of different extracting agents for a constant feed/solvent mass ratio. The process can either be considered as a batch or a continuous process. Eight common solvents from different chemical classes were considered as extracting agents; the essential requirement was that they exhibit a miscibility gap with water, which was the solvent in all studied mixtures, at the considered temperature, which was $T = 298.15$ K. The partitioning of all (pseudo-)components in thermodynamic equilibrium was calculated based on the isoactivity criterion:

$$x_i{}' \ \gamma_i{}'(T, \boldsymbol{x}') = x_i{}'' \ \gamma_i{}''(T, \boldsymbol{x}''); \quad i = 1...N \tag{1}$$

where $x_i{}'$ and $x_i{}''$ are the mole fraction of (pseudo-)component i in the raffinate (water-rich phase′) and the extract (extracting agent-rich phase″). $\gamma_i{}'$ and $\gamma_i{}''$ are the activity coefficients in the raffinate and extract phase, respectively, which were calculated using UNIFAC[3,4] based on the estimated composition for the poorly specified mixtures. For comparison only, all calculations were also carried out using the true composition of the studied mixtures. Numerical details for the calculations are given in the Supporting Information.

Prediction of Residue Curves

Residue curves are often used to model single-stage open evaporations, where the vapor phase is continuously removed. The residue curve thereby describes the composition of the liquid phase over time, which is considered to be always in thermodynamic equilibrium with the removed vapor phase.[45] This process is described by the Rayleigh-equation.[46,47] The pressure was 1 bar in all calculations in the present study.

In all cases, the vapor phase was treated as a mixture of ideal gases. Furthermore, the pressure dependence of the chemical potential in the liquid phase was always neglected. The vapor-liquid equilibrium was therefore modeled by extended Raoult's law:

$$p_i^{\mathrm{S}}(T) \ x_i \ \gamma_i(T, \boldsymbol{x}) = p \ y_i = p_i; \quad i = 1...N \tag{2}$$

where p_i^{S} is the vapor pressure of the pure component i, x_i and y_i are the mole fraction of i in the liquid and vapor phase in equilibrium, respectively, and p_i is the partial pressure of component i in the vapor phase. The activity coefficients γ_i in the liquid phase were again calculated with UNIFAC.[3,4]

For the fully specified mixtures, which were modeled as a reference here only, the vapor pressure of the pure components p_i^{S} was calculated using the Antoine equation with parameters taken from the Dortmund Data Bank (DDB).[48] Some of the considered components have very low vapor pressures, so that no data were available. In these cases, the vapor pressure of the component was set to zero, cf. Supporting Information for details.

For the poorly specified mixtures, the vapor pressure p_k^{S} of the pseudo-component k was estimated using the group-contribution method of Refs.[38,39] If the estimated vapor pressure was $p_k^{\mathrm{S}} < 10^{-10}$ bar at $T = 373$ K, it was set to zero. A detailed description of the calculation of the vapor pressures is given in the Supporting Information.

Overview of Studied Mixtures

Table 2 gives an overview of the three mixtures that were considered as feed mixtures in the application examples studied in the present work. The information on the feed mixtures was adopted from Ref.[18] - no NMR experiments were carried out in the present work. All mixtures are aqueous solutions that contain a cocktail of diluted substances (the mole fractions of all other components were below 0.038 mol/mol) - a situation that is often encountered, e.g., in biotechnological processes. We emphasize that the general methodology proposed here is not limited to such mixtures, and we plan to demonstrate the applicability to other types of poorly specified mixtures in future work.

The fact that diluted aqueous mixtures were studied has several consequences for the application of the methodology. Firstly, it explains why the study was carried out with ^{13}C NMR spectroscopy. Secondly, the high dilution poses challenges for spectroscopy, which can,

however, be overcome by sufficiently long measuring times. In the present work, the lowest solute concentration was about 0.006 mol/mol, cf. Table 2, for which a successful quantification of the structural groups was still possible.[18] A general indicator for the expected uncertainty of the integration is the signal-to-noise ratio (SNR), which depends, among other things, also on the used NMR device and experimental parameters like the number of scans. On the other hand, the high dilution in the solvent water facilitates the application of the SEGWE model for predicting diffusion coefficients at infinite dilution in a known solvent. As the concentration dependence of diffusion coefficients can be very strong, it was not neglected, despite the low concentrations of the solutes. To account for it, a reference component was used. For details, see Ref.[18] The reference components were randomly chosen in the three studied mixtures.

In the application examples that were studied here, we simply assume that the reference component is the component to be separated from the unknown mixture. This is motivated by the fact that in separation processes with poorly specified mixtures, the target component to be separated is always known - and also its concentration in the feed mixture is usually known. As the focus of the present study is on the application side, the reference component is labeled with T (target) in the following, cf. Table 2.

The fact that a priori information on the solvent and a reference component was used does not indicate a general limitation of the methodology: if this information is not directly available, samples of poorly specified mixtures can, in general, be diluted with a known inert solvent and also a reference component can be added gravimetrically.

Table 2: Overview of the mixtures studied in this work. All mixtures are diluted aqueous solutions; the solvent water is not explicitly included in the table. x_i and M_i are the mole fraction and the molar mass of the true components i, respectively, which were known from the preparation of the samples; x_i^{pred} and M_i^{pred} are corresponding numbers for the pseudo-components $\tilde{\text{U}}$ predicted based on NMR fingerprinting. The dashed lines indicate which true components were lumped into the pseudo-components by our approach. Target components are labeled with (T), see text.

Mixture	Components i	M_i / g mol^{-1}	M_i^{pred} / g mol^{-1}	x_i / mol mol^{-1}	x_i^{pred} / mol mol^{-1}
I	2-propanol (T)	60.10	-	0.033	0.034
	acetone ($\tilde{\text{U}}_1$)	58.08	48.98	0.038	0.046
	1,4-butanediol ($\tilde{\text{U}}_2$)	90.12	145.21	0.035	0.022
	acetic acid ($\tilde{\text{U}}_3$)	60.05	72.11	0.033	0.029
II	1,4-dioxane (T)	88.11	-	0.006	0.006
	cyclohexanone ($\tilde{\text{U}}_1$)	98.15	94.47	0.012	0.012
	glucose ($\tilde{\text{U}}_2$)	180.16	212.08	0.015	0.034
	citric acid ($\tilde{\text{U}}_2$)	192.12		0.025	
III	acetonitrile (T)	41.05	-	0.022	0.022
	acetone ($\tilde{\text{U}}_1$)	58.08	51.71	0.016	0.017
	acetic acid ($\tilde{\text{U}}_2$)	60.05	71.06	0.015	0.013
	1-propanol ($\tilde{\text{U}}_3$)	60.10	85.26	0.015	0.021
	2-propanol ($\tilde{\text{U}}_3$)	60.10		0.015	
	cyclohexanone ($\tilde{\text{U}}_4$)	98.15	115.96	0.009	0.007
	1,4-butanediol ($\tilde{\text{U}}_5$)	90.12	148.90	0.010	0.006
	malic acid ($\tilde{\text{U}}_6$)	134.09	248.36	0.008	0.009
	xylose ($\tilde{\text{U}}_6$)	150.13		0.007	
	ascorbic acid ($\tilde{\text{U}}_7$)	176.12	313.85	0.006	0.004

Additional results for the quantification of the structural groups based on NMR fingerprinting are presented in the Supporting Information.

The results presented in Table 2 show that the NMR fingerprinting in combination with the pseudo-component method works well. The true compositions of the mixtures and the respective predicted compositions agree well in most cases. There are considerable discrepancies in the predicted molar masses of some components that are, however, mainly caused by deficiencies of the SEGWE[35,36] model, as shown in Ref.[18] In the SEGWE model, the only property of the solute that is taken into account for the prediction of the molar mass is the solute's self-diffusion coefficient. On the one hand, this simplicity makes the SEGWE model attractive. On the other hand, improvements might be obtained by, e.g., considering information on the chemical nature of the solute in the diffusion model. Hence, developing advanced methods for predicting diffusion coefficients would be highly desirable also for the present methodology. Still, the good agreement of the predicted and the true compositions shows that the method works well also with the SEGWE model. It is noted that for the components labeled with ($\tilde{\mathrm{U}}$) in Table 2, no information on the true nature and concentration was used to determine the predicted values, whereas, as explained above, for the target components (T), the mass fraction and the nature was assumed to be known. Still, as the predicted molar masses are used for the prediction of the mole fractions, also the mole fraction of the target component T is a prediction, albeit a much simpler one than for the other components $\tilde{\mathrm{U}}$. Since water and the target component were assumed to be known here, they were treated as true components in the calculations (e.g., using Antoine parameters from the DDB[48] for calculating the vapor pressure).

Results and Discussion

Solvent Screening for Liquid-liquid Extraction Processes

The simulation study of liquid-liquid extraction processes with poorly specified feeds that was carried out in the present work represents the scenario of a solvent screening. The aim of the processes is to remove a known target component T from a poorly specified aqueous mixture by an extracting agent E, which has to be selected from a list of candidates. For simplicity, both the temperature and the mass ratio of the extracting agent and the feed were kept constant and set to $T = 298.15$ K and $m_{\mathrm{E}}/m_{\mathrm{F}} = 5$, respectively. However, our approach easily generalizes to other temperatures and mass ratios. Eight common solvents that have a wide miscibility gap with water were considered as extracting agents: 1-octanol, 1-decanol, toluene, hexane, decane, dipropyl ether, ethyl propionate, and 3-octanone. The extension to other extracting agents is straightforward.

The selectivity is quantified by the separation factor α_{T} of the target component, which compares the distribution of the target component on the coexisting phases in thermodynamic equilibrium with the respective distributions of all identified pseudo-components $\tilde{\mathrm{U}}_k$:

$$\alpha_{\mathrm{T}} = \frac{\left(\frac{x''_{\mathrm{T}}}{x'_{\mathrm{T}}}\right)}{\left(\frac{\sum_{k=1}^{K} x''_{\tilde{\mathrm{U}}_k}}{\sum_{k=1}^{K} x'_{\tilde{\mathrm{U}}_k}}\right)} \tag{3}$$

where the double prime indicates the extract phase and the prime denotes the raffinate phase. The numerator is the partition coefficient of the target component and the denominator is the partition coefficient of all other components (except water) lumped together. The yield is:

$$Y_{\mathrm{T}} = \frac{n''_{\mathrm{T}}}{n'_{\mathrm{T}} + n''_{\mathrm{T}}} \tag{4}$$

where n_{T} refers to the mole number of the target component. For comparison, these quantities were also calculated for the fully specified mixtures, i.e., using the complete knowledge

of the composition of the mixtures, cf. Table 2. These results are called ground truth in the following.

In Figure 2, the results for the extraction of the target component T=2-propanol from mixture I (cf. Table 2), are shown. A very good agreement between the predictions (open symbols) and the ground truth (closed symbols) is found for all extracting agents; this holds for both the separation factor α_{T} (Figure 2 left) and the extraction yield Y_{T} (Figure 2 right).

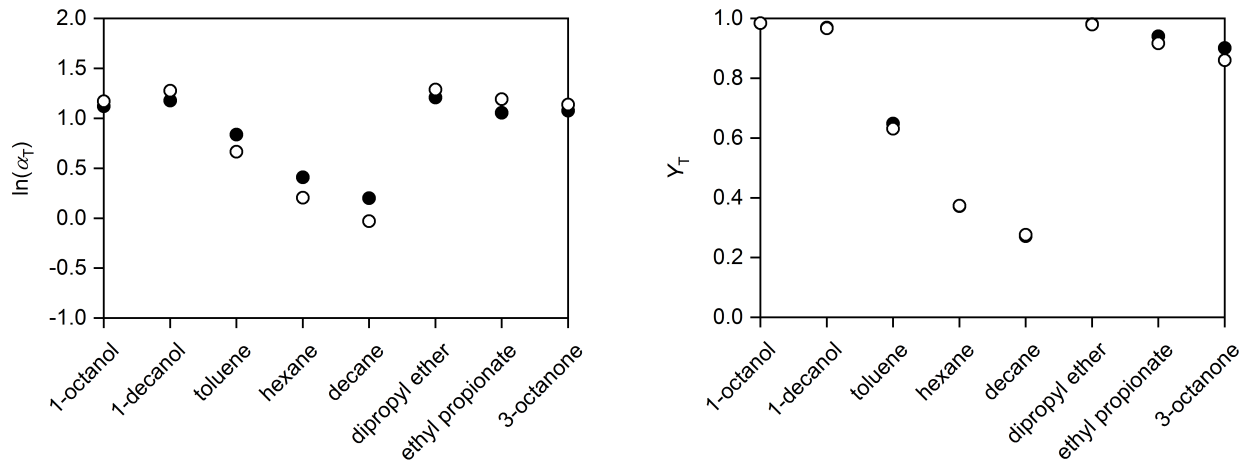

Figure 2: Separation factor α_{T} (left) and extraction yield Y_{T} (right) of target component T=2-propanol in a single-stage liquid-liquid extraction process with mixture I (cf. Table 2), as feed F for different extracting agents E at $T = 298.15$ K and $m_{\mathrm{E}}/m_{\mathrm{F}} = 5$. Closed symbols: results for the fully specified feed. Open symbols: predictions for the poorly specified feed using NMR fingerprinting and the pseudo-component method. In some cases, the prediction is so good that the two symbols become indistinguishable.

Figure 3 shows the corresponding results for extracting the target component T=1,4-dioxane from mixture II. Again, for both the separation factor α_{T} (Figure 3 left) and the extraction yield Y_{T} (Figure 3 right), excellent agreement between the predictions (open symbols) and the ground truth (closed symbols) is found for all extracting agents. Note that the pseudo-component method could not distinguish glucose and citric acid here, which were lumped into a single pseudo-component ($\tilde{\mathrm{U}}_2$), cf. Table 2. The fact that, nevertheless, good results were obtained demonstrates that the approach is robust with respect to the definition of the pseudo-components. We assume that this is because the clustering of the identified structural groups is based on physics, namely on information on self-diffusion coefficients.

While glucose and citric acid are chemically different, they differ not so much regarding their interactions with water and their molar mass.

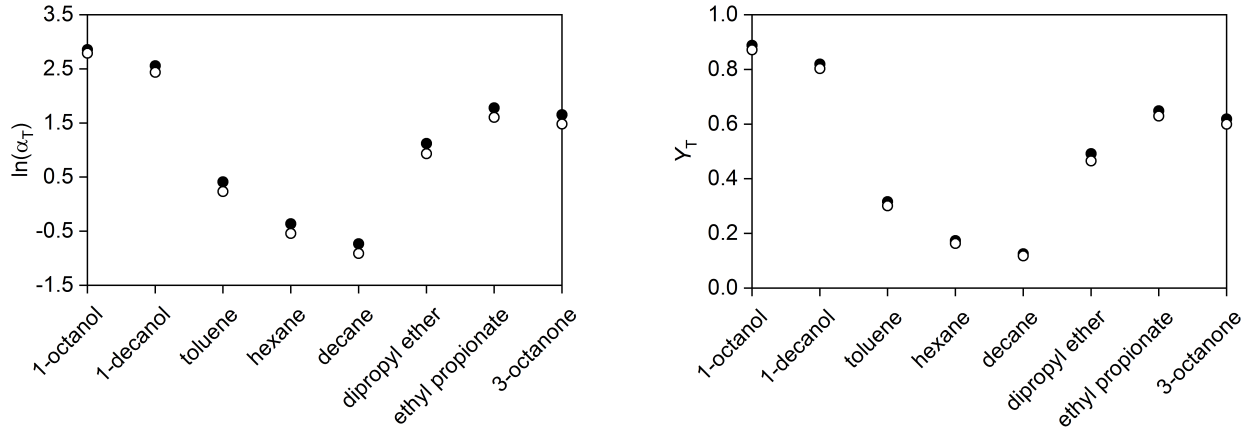

Figure 3: Separation factor α_{T} (left) and extraction yield Y_{T} (right) of target component T=1,4-dioxane in a single-stage liquid-liquid extraction process with mixture II (cf. Table 2), as feed F for different extracting agents E at $T = 298.15$ K and $m_{\mathrm{E}}/m_{\mathrm{F}} = 5$. Closed symbols: results for the fully specified feed. Open symbols: predictions for the poorly specified feed using NMR fingerprinting and the pseudo-component method.

In Figure 4, the results for mixture III with the target component T=acetonitrile are shown. For both the separation factor α_{T} (Figure 4 left) and the extraction yield of the target component Y_{T} (Figure 4 right), excellent agreement between the ground truth and the predictions is found for all studied extracting agents. In some cases, the differences are even indistinguishable in Figure 4. This is particularly interesting since the mixture contains nine components that were assumed to be unknown, which were lumped into a total of seven pseudo-components by our algorithms, cf. Table 2. Again, this shows the robustness of the approach.

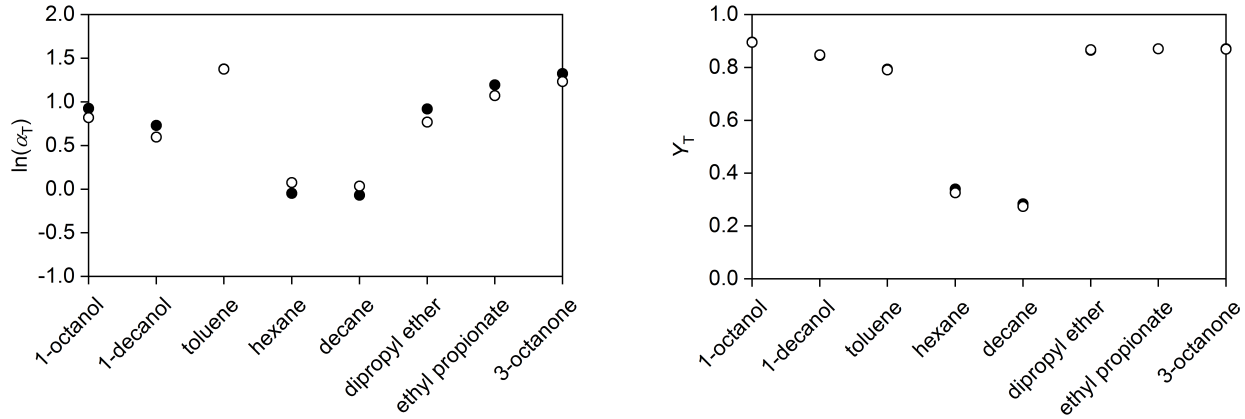

Figure 4: Separation factor α_{T} (left) and extraction yield Y_{T} (right) of target component T=acetonitrile in a single-stage liquid-liquid extraction process with mixture III (cf. Table 2), as feed F for different extracting agents E at $T = 298.15$ K and $m_{\mathrm{E}}/m_{\mathrm{F}} = 5$. Closed symbols: results for the fully specified feed. Open symbols: predictions for the poorly specified feed using NMR fingerprinting and the pseudo-component method. In some cases, the prediction is so good that the two symbols become indistinguishable.

Simulation of Open Evaporation Processes

In the following, results for an open evaporation process are shown. The results are presented over the evaporation ratio β:

$$\beta = 1 - \frac{n^{\mathrm{L}}}{n^{\mathrm{L},0}} \tag{5}$$

where n^{L} is the number of moles in the residue and $n^{\mathrm{L},0}$ the initial value of that property. The simulations were performed until the number of moles n^{L} in the residue approached the total amount of non-volatile components; cf. Supporting Information for details.

Figure 5 shows the boiling temperature T of the three test mixtures during the open evaporation process at $p = 1$ bar. The overall agreement of the calculations for the fully specified mixtures (solid lines) with the predictions based on NMR fingerprinting and the pseudo-component method (dashed lines) is good in all cases. However, for mixture I, the boiling temperature is underestimated for low evaporation ratios, which is presumably because the vapor pressure of $\tilde{\mathrm{U}}_1$ (representing acetone, cf. Table 2) is overestimated. The influence of $\tilde{\mathrm{U}}_1$ on the boiling temperature is then reduced due to its fast evaporation, cf. also Figure 6. In the Supporting Information, the predicted vapor pressures of the

pseudo-components based on the group-contribution method used here[38,39] are compared to the vapor pressures as calculated by the Antoine equation. In general, considerable differences were obtained between these two calculations, which is presumably a two-fold problem: first, the prediction accuracy of the molar masses is not sufficient in some cases, and second, the group-contribution method for the prediction of the vapor pressure is not accurate enough. However, the impact of these false predictions is moderate as the order in which the components evaporate is correctly described in most cases, cf. Figures S.1-S.3 in the Supporting Information, and the qualitative behavior of the vapor pressure curves are well predicted.

Furthermore, in mixtures I and III, relatively high temperatures are predicted for high evaporation ratios; in mixture I, this is mainly caused by pseudo-component $\tilde{\mathrm{U}}_2$ (representing 1,4-butanediol, cf. Table 2), for which the vapor pressure is underestimated, cf. Figure S.1 in the Supporting Information. In mixture III, for high evaporation ratios, the non-volatile components malic acid, xylose, and ascorbic acid accumulate in the liquid phase.

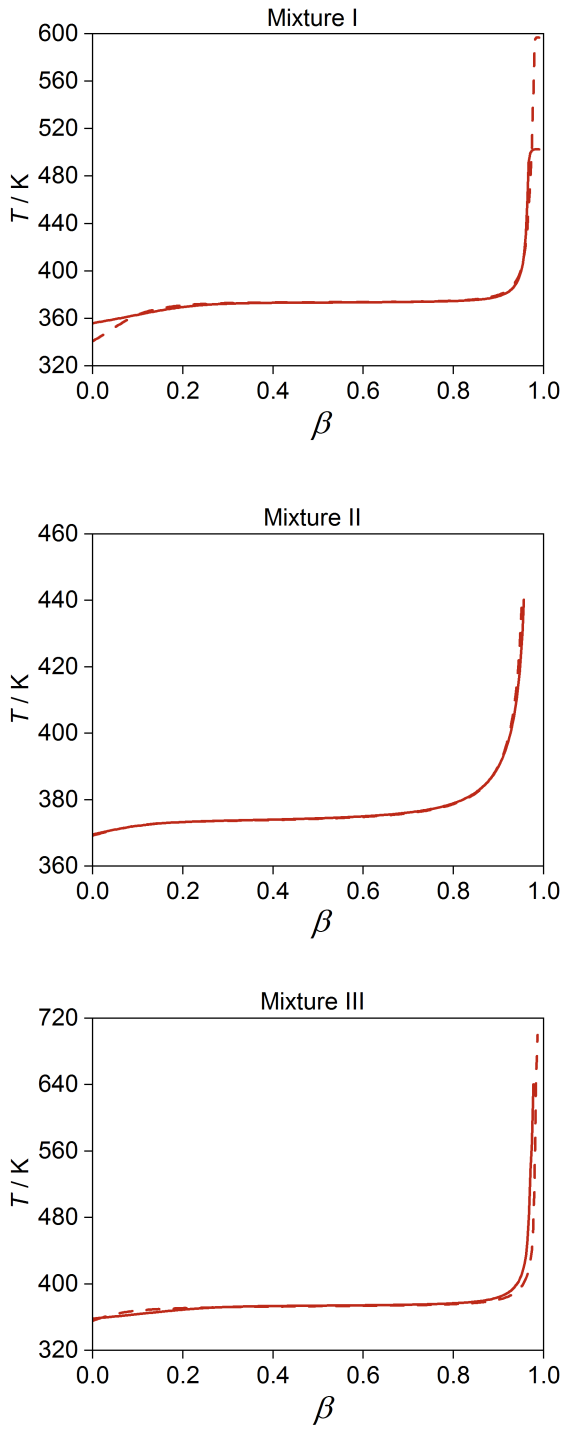

Figure 5: Results from simulations of open evaporation processes at 1 bar for mixtures I - III (cf. Table 2). The boiling temperature T is shown as a function of the evaporation ratio β. Solid lines: results for the fully specified mixtures. Dashed lines: predictions for the poorly specified mixtures based on NMR fingerprinting and the pseudo-component method.

Figure 6 shows the residue curves, i.e., the mole fractions of the components in the liquid phase over the course of the process, for mixture I at $p = 1$ bar (cf. Table 2). In the left panel, results for the fully specified mixture are shown, the right panel shows the corresponding results obtained from NMR fingerprinting and the pseudo-component method. Overall, the predictions agree well with the results obtained using the complete speciation of the feed. The imperfect prediction of the composition of the feed (at $\beta = 0$) is mainly caused by errors in the prediction of the molar masses. For instance, the underestimation of the molar mass of acetone (represented by $\tilde{\mathrm{U}}_1$) leads to an overestimation of its mole fraction. Similarly, the mole fraction of acetic acid is underestimated because its molar mass is overestimated.

The maximum in the residue curve of acetic acid is also found for the pseudo-component $\tilde{\mathrm{U}}_3$, which represents acetic acid, but the maximum is by far overpredicted. This is presumably a consequence of the overprediction of the molar mass of acetic acid and problems of the group-contribution method used to predict the vapor pressure of that component (cf. Figure S.1 in the Supporting Information).

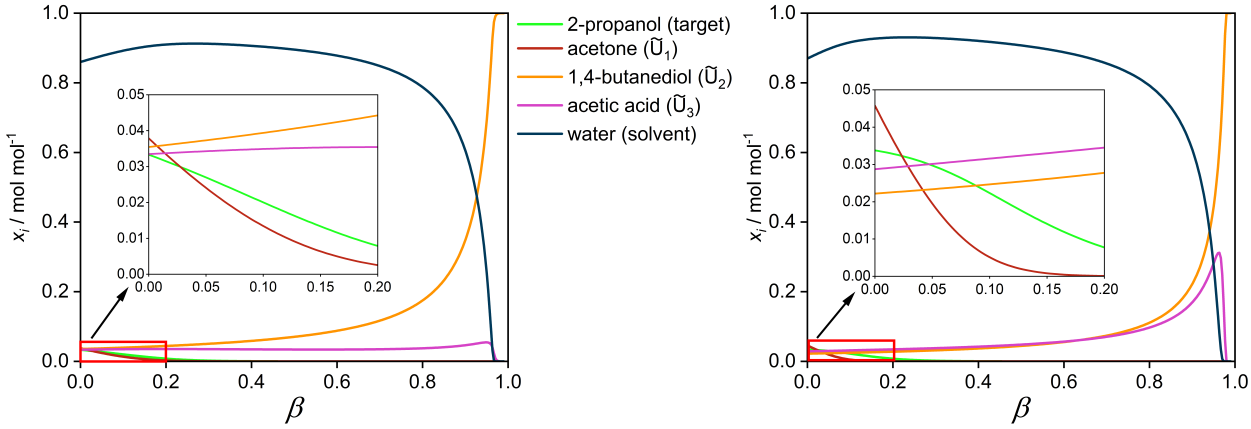

Figure 6: Residue curves showing the liquid-phase mole fractions x_i as a function of the evaporation ratio β for mixture I (cf. Table 2), at $p = 1$ bar. Left: results obtained using the full speciation. Right: predictions based on NMR fingerprinting and the pseudo-component method.

Figure 7 shows the respective results for the residue curves for mixture II. The agreement between the predicted residue curves and the ones calculated using the complete information on the composition of the mixture is excellent for all components. Citric acid and glucose

were lumped into a single pseudo-component ($\tilde{U}_2$), cf. Table 2; therefore, only the sum of the mole fractions of both components is indicated in both panels of Figure 7. A representation with individual mole fractions is shown in Figure S.4 in the Supporting Information.

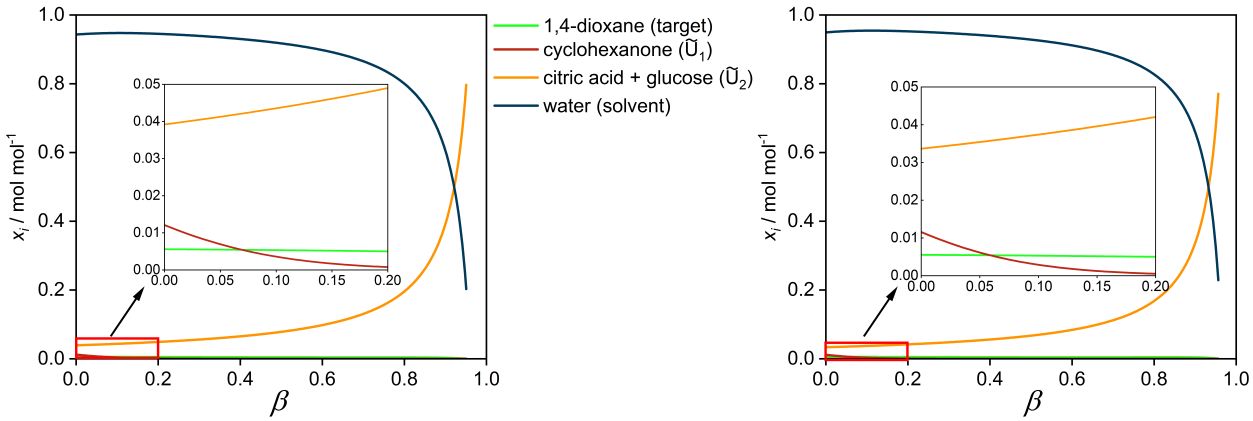

Figure 7: Residue curves showing the liquid-phase mole fractions x_i as a function of the evaporation ratio β for mixture II (cf. Table 2), at $p = 1$ bar. Left: results obtained using the full speciation. Right: predictions based on NMR fingerprinting and the pseudo-component method.

We note that the concentrations of citric acid and glucose in the liquid phase for high evaporation ratios are so high that, in practice, they would precipitate, i.e., an additional solid-liquid equilibrium (SLE) would occur, which, however, was not considered here.

Figure 8 shows the respective residue curves for mixture III. A good agreement between the predicted residue curves and those obtained using the full speciation is found for most components. While the maximum in the concentration curve of 1,4-butanediol ($\tilde{U}_5$) is well predicted, as for mixture I, poor results are obtained for acetic acid ($\tilde{U}_2$), for which a strong maximum is predicted, which is not found when the full speciation is used. The reasons are the same as for mixture I: the poor prediction of the molar mass and the vapor pressure. 1-propanol and 2-propanol were lumped into a single pseudo-component ($\tilde{U}_3$); the same holds for malic acid and xylose ($\tilde{U}_6$), cf. Table 2. Therefore, only the sums of the mole fractions of the respective true components are plotted in these cases, cf. Figure S.5 in the Supporting Information for a plot of the individual concentrations. The lumping of 1-propanol and 2-propanol is a good example for a lumping that is uncritical for the prediction

of thermophysical properties. Also, the lumping of the two high-boilers, malic acid and xylose, does not substantially affect the prediction of residue curves. As with mixture II, the possible occurrence of an SLE was not considered here, although it might occur in practice for high evaporation ratios.

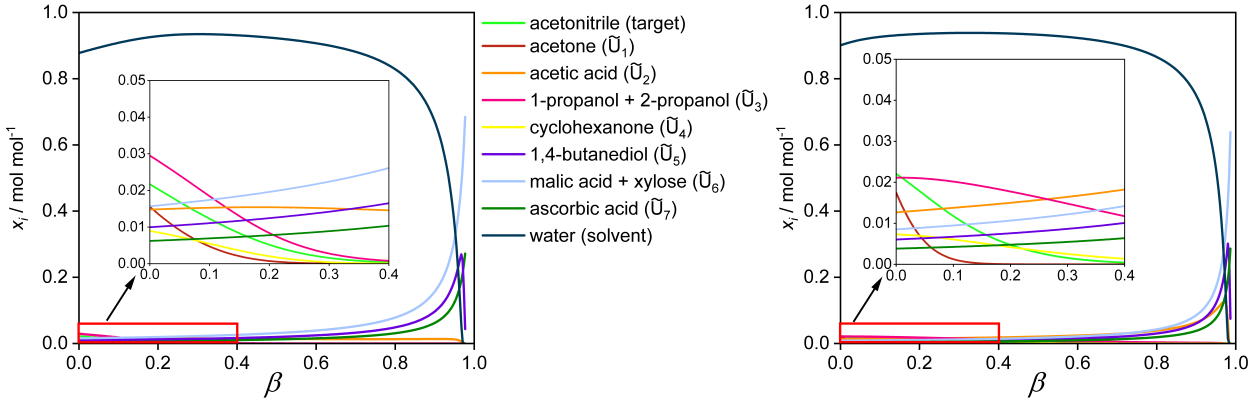

Figure 8: Residue curves showing the liquid-phase mole fractions x_i as a function of the evaporation ratio β for mixture III (cf. Table 2), at $p = 1$ bar. Left: results obtained using the full speciation. Right: predictions based on NMR fingerprinting and the pseudo-component method.

Conclusions

In this work, we have demonstrated that predictive thermodynamic modeling can be achieved without knowing the full speciation of the mixtures. The basic idea is simple: we use NMR spectroscopy to obtain a fingerprint of the poorly specified mixture, i.e., for obtaining quantitative information on its group composition (which is much easier than getting the full speciation). Then we define pseudo-components based on information on diffusion coefficients from PFG NMR spectroscopy and use this information also for determining the molar mass of the pseudo-components using the SEGWE[35,36] model. This gives us all we need to apply thermodynamic group-contribution models to predict the properties of the poorly specified mixture. This concept has been established in a previous paper[18] and was applied here for the first time to chemical engineering problems. Two examples were studied: the

simulation of liquid-liquid extraction processes in a solvent-screening scenario and the simulation of open evaporation processes by the prediction of residue curves. In all cases, the predictions for the poorly specified feeds were compared to results obtained using the knowledge of the complete speciation of the mixtures, and excellent agreement was found. The results show that the proposed methodology is a valuable tool for thermodynamic modeling and simulation and allows reliable predictions without the need for elaborate component elucidation of the full speciation.

The approach was only applied to aqueous mixtures, but there is no reason why it could not be applied to non-aqueous solutions. On the contrary: for non-aqueous solutions, it could be attractive to combine the information from ^{13}C NMR spectroscopy that was used here with that from ^{1}H NMR spectroscopy, which could further improve the results. Also, variants based solely on ^{1}H NMR spectroscopy could be developed. The clustering of the structural groups to pseudo-components currently relies only on measured self-diffusion coefficients; as a result, components with very similar diffusion coefficients can be lumped into one pseudo-component. To address this, e.g., the number of gradient steps and, thereby, the resolution of the PFG NMR experiments can be increased, but also prior knowledge can be incorporated if available.[18] Furthermore, in future work, new NMR methods could be employed, e.g., the REST[49] method, which relies on relaxation encoding.

Furthermore, only mixtures were studied in which the components were highly diluted in the solvent (always water here). This is no prerequisite for applying the NMR fingerprinting and the definition of pseudo-components, but the absence of a component that is present in large excess troubles the determination of the molar mass of the pseudo-components. If such an excess component is not present, it can be added. The prerequisite for this would be that the added component is miscible with the poorly specified mixture and non-reactive. Furthermore, it is desirable to have one component of which the concentration is known. This will be the case in most practical problems with poorly specified mixtures, e.g., the concentration of a product in an otherwise poorly specified mixture. If this was not the

case, such a component could be added to the mixture. In the present paper, this reference component was designated.

The method depends on the quality of prediction methods that are needed at two points: firstly, the SEGWE model for predicting diffusion coefficients is used to get the information on the molar mass of the pseudo-components, and secondly, group-contribution methods are used to predict the thermodynamic properties of interest. The quality of the latter methods directly limits what can be achieved with the present approach. Luckily, many suitable thermodynamic group-contribution methods are available for a large variety of properties. Applying these methods in the present framework requires mapping the groups that can be identified by NMR spectroscopy to groups considered in the thermodynamic method. This may require some case-specific adaptions but will hardly pose fundamental problems. We emphasize that also the flexibility on the NMR spectroscopic side can be used for such adaptions and that we expect to see progress in the group assignment in NMR spectroscopy by using machine learning.[50]

The results from the present examples also show that even the best available semi-empirical methods for predicting diffusion coefficients[37] (the SEGWE model[35,36]) and a well-developed method for predicting pure-component vapor pressures (the method of Refs.[38,39]) have critical deficiencies. Some of the most critical deviations observed in comparing our predictions to those obtained using the full speciation resulted from deficiencies of these models and not directly from the methodology presented here; hence, our methodology will strongly profit from any future improvement of these models.

The present results were obtained based on NMR experiments with cryogenic high-field instruments. In future work, the methodology should be adapted to use results from much simpler and cheaper benchtop NMR spectrometers. Furthermore, the present work demonstrates that the approach developed in Ref.[18] to solve the problem of modeling poorly specified mixtures is broadly applicable. It is also flexible and can be tuned to specific needs. More studies should follow to elucidate and demonstrate the full potential of the new approach.

Acknowledgement

F.J. gratefully acknowledges financial support from Deutsche Forschungsgemeinschaft (DFG) under Grant No JI 401/1-1.

Supporting Information Available

Supporting Information is available free of charge at [Link]:

- Calculation of liquid-liquid equilibria
- Prediction of residue curves
- Prediction of feed composition
- Predicted composition of pseudo-components
- Results for pure-component vapor pressures
- Additional results for the prediction of residue curves

References

(1) Renon, H.; Prausnitz, J. M. Local Compositions in Thermodynamic Excess Functions for Liquid Mixtures. *AIChE Journal* **1968**, *14*, 135–144, DOI: `10.1002/aic.690140124`.

(2) Abrams, D. S.; Prausnitz, J. M. Statistical Thermodynamics of Liquid Mixtures: A New Expression for the Excess Gibbs Energy of Partly or Completely Miscible Systems. *AIChE Journal* **1975**, *21*, 116–128, DOI: `10.1002/aic.690210115`.

(3) Fredenslund, A.; Jones, R. L.; Prausnitz, J. M. Group-Contribution Estimation of Activity Coefficients in Nonideal Liquid Mixtures. *AIChE Journal* **1975**, *21*, 1086–1099, DOI: `10.1002/aic.690210607`.

(4) Wittig, R.; Lohmann, J.; Gmehling, J. Vapor-Liquid Equilibria by UNIFAC Group Contribution. 6. Revision and Extension. *Industrial & Engineering Chemistry Research* **2003**, *42*, 183–188, DOI: 10.1021/ie0205061.

(5) Alexander, G. L.; Schwarz, B. J.; Prausnitz, J. M. Phase Equilibriums for High-boiling Fossil Fuel Distillates. 2. Correlation of Equation-of-state Constants with Characterization Data for Phase Equilibrium Calculations. *Industrial & Engineering Chemistry Fundamentals* **1985**, *24*, 311–315, DOI: 10.1021/i100019a006.

(6) Carreón-Calderón, B.; Uribe-Vargas, V.; Ramírez-Jaramillo, E.; Ramírez-de Santiago, M. Thermodynamic Characterization of Undefined Petroleum Fractions using Group Contribution Methods. *Industrial & Engineering Chemistry Research* **2012**, *51*, 14188–14198, DOI: 10.1021/ie3016076.

(7) Cuellar, M. C.; Straathof, A. J. Downstream of the Bioreactor: Advancements in Recovering Fuels and Commodity Chemicals. *Current Opinion in Biotechnology* **2020**, *62*, 189–195, DOI: 10.1016/j.copbio.2019.11.012.

(8) Guellil, A.; Thomas, F.; Block, J.-C.; Bersillon, J.-L.; Ginestet, P. Transfer of Organic Matter Between Wastewater and Activated Sludge Flocs. *Water Research* **2001**, *35*, 143–150, DOI: 10.1016/S0043-1354(00)00240-2.

(9) Sim, W. J.; Daubert, T. E. Prediction of Vapor-Liquid Equilibria of Undefined Mixtures. *Industrial & Engineering Chemistry Process Design and Development* **1980**, *19*, 386–393, DOI: 10.1021/i260075a010.

(10) Fahim, M. A.; Elkilani, A. S. Prediction of Solubility of Hydrogen in Petroleum Cuts using Modified Unifac. *The Canadian Journal of Chemical Engineering* **1992**, *70*, 335–340, DOI: 10.1002/cjce.5450700218.

(11) Gao, Z.; Xu, Z.; Zhao, S.; Zhang, L. Heavy Petroleum Supercritical Fluid Deasphalting

Process Simulation Based On the Saturate, Aromatic, Resin, and Asphaltene Composition. *Energy & Fuels* **2022**, *36*, 8818–8827, DOI: 10.1021/acs.energyfuels.2c00891.

(12) Rätzsch, M. T.; Kehlen, H. Continuous Thermodynamics of Polymer Solutions: The Effect of Polydispersity on the Liquid-Liquid Equilibrium. *Journal of Macromolecular Science: Part A - Chemistry* **1985**, *22*, 323–334, DOI: 10.1080/00222338508056606.

(13) Rätzsch, M. T.; Kehlen, H.; Browarzik, D. Liquid-Liquid Equilibrium of Polydisperse Copolymer Solutions. Multivariate Distribution Functions in Continuous Thermodynamics. *Journal of Macromolecular Science: Part A - Chemistry* **1985**, *22*, 1679–1690, DOI: 10.1080/00222338508063365.

(14) Cotterman, R. L.; Bender, R.; Prausnitz, J. M. Phase Equilibria for Mixtures Containing Very Many Components. Development and Application of Continuous Thermodynamics for Chemical Process Design. *Industrial & Engineering Chemistry Process Design and Development* **1985**, *24*, 194–203, DOI: 10.1021/i200028a033.

(15) Fang, W.; Lei, Q. Continuous Thermodynamic Correlation and Calculation of Vapor Pressure and Vapor–liquid Equilibrium Constant of Hydrocarbon Fuel Fractions. *Fluid Phase Equilibria* **2003**, *213*, 125–138, DOI: 10.1016/S0378-3812(03)00238-3.

(16) Liu, L.; Hou, S.; Zhang, N. Incorporating Numerical Molecular Characterization into Pseudo-component Representation of Light to Middle Petroleum Distillates. *Chemical Engineering Science: X* **2019**, *3*, 100029, DOI: 10.1016/j.cesx.2019.100029.

(17) Gómez-Siurana, A.; Font-Escamilla, A.; García-Soler, C. Learning about Distillation Curves as a Way to Define a Process Stream from Crude Petroleum. *Education for Chemical Engineers* **2019**, *26*, 35–40, DOI: 10.1016/j.ece.2018.11.001.

(18) Specht, T.; Münnemann, K.; Hasse, H.; Jirasek, F. Rational Method for Defining and Quantifying Pseudo-components Based on NMR Spectroscopy. *Physical Chemistry Chemical Physics* **2023**, *25*, 10288–10300, DOI: 10.1039/d3cp00509g.

(19) Jirasek, F.; Burger, J.; Hasse, H. Method for Estimating Activity Coefficients of Target Components in Poorly Specified Mixtures. *Industrial & Engineering Chemistry Research* **2018**, *57*, 7310–7313, DOI: 10.1021/acs.iecr.8b00917.

(20) Jirasek, F.; Burger, J.; Hasse, H. NEAT—NMR Spectroscopy for the Estimation of Activity Coefficients of Target Components in Poorly Specified Mixtures. *Industrial & Engineering Chemistry Research* **2019**, *58*, 9155–9165, DOI: 10.1021/acs.iecr.9b01269.

(21) Jirasek, F.; Burger, J.; Hasse, H. Application of NEAT for Determining the Composition Dependence of Activity Coefficients in Poorly Specified Mixtures. *Chemical Engineering Science* **2019**, *208*, 115161, DOI: 10.1016/j.ces.2019.115161.

(22) Jirasek, F.; Burger, J.; Hasse, H. Application of NEAT for the Simulation of Liquid–liquid Extraction Processes with Poorly Specified Feeds. *AIChE Journal* **2020**, *66*, e16826, DOI: https://doi.org/10.1002/aic.16826.

(23) Specht, T.; Münnemann, K.; Jirasek, F.; Hasse, H. Estimating Activity Coefficients of Target Components in Poorly Specified Mixtures with NMR Spectroscopy and COSMO-RS. *Fluid Phase Equilibria* **2020**, *516*, 112604, DOI: 10.1016/j.fluid.2020.112604.

(24) Spraul, M.; Schütz, B.; Humpfer, E.; Mörtter, M.; Schäfer, H.; Koswig, S.; Rinke, P. Mixture Analysis by NMR as applied to Fruit Juice Quality Control. *Magnetic Resonance in Chemistry* **2009**, *47*, S130–S137, DOI: 10.1002/mrc.2528.

(25) McKenzie, J. S.; Donarski, J. A.; Wilson, J. C.; Charlton, A. J. Analysis of Complex Mixtures using High-resolution Nuclear Magnetic Resonance Spectroscopy and Chemometrics. *Progess in Nuclear Magnetic Resonance Spectroscopy* **2011**, *59*, 336–359, DOI: 10.1016/j.pnmrs.2011.04.003.

(26) van Duynhoven, J.; van Velzen, E.; Jacobs, D. M. *Annual Reports*

on NMR Spectroscopy; Academic Press, 2013; pp 181–236, DOI: 10.1016/b978-0-12-408097-3.00003-2.

(27) Schievano, E.; Tonoli, M.; Rastrelli, F. NMR Quantification of Carbohydrates in Complex Mixtures. A Challenge on Honey. *Analytical Chemistry* **2017**, *89*, 13405–13414, DOI: 10.1021/acs.analchem.7b03656.

(28) Behrens, R.; Kessler, E.; Münnemann, K.; Hasse, H.; von Harbou, E. Monoalkylcarbonate Formation in the System Monoethanolamine–Water–Carbon Dioxide. *Fluid Phase Equilibria* **2019**, *486*, 98–105, DOI: 10.1016/j.fluid.2018.12.031.

(29) Fröscher, A.; Langenbach, K.; von Harbou, E.; Thiel, W. R.; Hasse, H. NMR Spectroscopic Study of Chemical Reactions in Mixtures Containing Oleic Acid, Formic Acid, and Formoxystearic Acid. *Industrial & Engineering Chemistry Research* **2019**, *58*, 5622–5630, DOI: 10.1021/acs.iecr.8b05715.

(30) Vollhardt, K. P. C.; Schore, N. E. *Organic Chemistry: Structure and Function*, 8th ed.; Macmillan Learning: New York, 2018.

(31) Stejskal, E. O.; Tanner, J. E. Spin Diffusion Measurements: Spin Echoes in the Presence of a Time-Dependent Field Gradient. *The Journal of Chemical Physics* **1965**, *42*, 288–292, DOI: 10.1063/1.1695690.

(32) Bellaire, D.; Kiepfer, H.; Münnemann, K.; Hasse, H. PFG-NMR and MD Simulation Study of Self-Diffusion Coefficients of Binary and Ternary Mixtures Containing Cyclohexane, Ethanol, Acetone, and Toluene. *Journal of Chemical & Engineering Data* **2020**, *65*, 793–803, DOI: 10.1021/acs.jced.9b01016.

(33) Bellaire, D.; Großmann, O.; Münnemann, K.; Hasse, H. Diffusion Coefficients at Infinite Dilution of Carbon Dioxide and Methane in Water, Ethanol, Cyclohexane, Toluene, Methanol, and Acetone: A PFG-NMR and MD Simulation Study. *The Journal of Chemical Thermodynamics* **2022**, *166*, 106691, DOI: 10.1016/j.jct.2021.106691.

(34) Rousseeuw, P. J. Silhouettes: A Graphical Aid to the Interpretation and Validation of Cluster Analysis. *Journal of Computational and Applied Mathematics* **1987**, *20*, 53–65, DOI: 10.1016/0377-0427(87)90125-7.

(35) Evans, R.; Deng, Z.; Rogerson, A. K.; McLachlan, A. S.; Richards, J. J.; Nilsson, M.; Morris, G. A. Quantitative Interpretation of Diffusion-Ordered NMR Spectra: Can We Rationalize Small Molecule Diffusion Coefficients? *Angewandte Chemie International Edition* **2013**, *52*, 3199–3202, DOI: 10.1002/anie.201207403.

(36) Evans, R.; Poggetto, G. D.; Nilsson, M.; Morris, G. A. Improving the Interpretation of Small Molecule Diffusion Coefficients. *Analytical Chemistry* **2018**, *90*, 3987–3994, DOI: 10.1021/acs.analchem.7b05032.

(37) Großmann, O.; Bellaire, D.; Hayer, N.; Jirasek, F.; Hasse, H. Database for Liquid Phase Diffusion Coefficients at Infinite Dilution at 298 K and Matrix Completion Methods for their Prediction. *Digital Discovery* **2022**, *1*, 886–897, DOI: 10.1039/d2dd00073c.

(38) Nannoolal, Y.; Rarey, J.; Ramjugernath, D.; Cordes, W. Estimation of Pure Component Properties: Part 1. Estimation of the Normal Boiling Point of Non-electrolyte Organic Compounds via Group Contributions and Group Interactions. *Fluid Phase Equilibria* **2004**, *226*, 45–63, DOI: 10.1016/j.fluid.2004.09.001.

(39) Nannoolal, Y.; Rarey, J.; Ramjugernath, D. Estimation of Pure Component Properties: Part 3. Estimation of the Vapor Pressure of Non-Electrolyte Organic Compounds via Group Contributions and Group Interactions. *Fluid Phase Equilib.* **2008**, *269*, 117–133, DOI: 10.1016/j.fluid.2008.04.020.

(40) Nannoolal, Y.; Rarey, J.; Ramjugernath, D. Estimation of Pure Component Properties: Part 2. Estimation of Critical Property Data by Group Contribution. *Fluid Phase Equilibria* **2007**, *252*, 1–27, DOI: 10.1016/j.fluid.2006.11.014.

(41) Mu, T.; Rarey, J.; Gmehling, J. Group Contribution Prediction of Surface Charge Density Profiles for COSMO-RS(Ol). *AIChE Journal* **2007**, *53*, 3231–3240, DOI: 10.1002/aic.11338.

(42) Constantinescu, D.; Gmehling, J. Further Development of Modified UNIFAC (Dortmund): Revision and Extension 6. *Journal of Chemical & Engineering Data* **2016**, *61*, 2738–2748, DOI: 10.1021/acs.jced.6b00136.

(43) Sun, S.; Lü, L.; Yang, A.; Wei, S.; Shen, W. Extractive Distillation: Advances in Conceptual Design, Solvent Selection, and Separation Strategies. *Chinese Journal of Chemical Engineering* **2019**, *27*, 1247–1256, DOI: 10.1016/j.cjche.2018.08.018.

(44) Online Group Assignment for UNIFAC. http://www.ddbst.com/unifacga.html (Last accessed: 30.03.2023).

(45) Kiva, V.; Hilmen, E.; Skogestad, S. Azeotropic Phase Equilibrium Diagrams: a Survey. *Chemical Engineering Science* **2003**, *58*, 1903–1953, DOI: 10.1016/S0009-2509(03)00018-6.

(46) Rayleigh, L. LIX. On the Distillation of Binary Mixtures. *The London, Edinburgh, and Dublin Philosophical Magazine and Journal of Science* **1902**, *4*, 521–537, DOI: 10.1080/14786440209462876.

(47) Stichlmair, J.; Klein, H.; Rehfeldt, S. *Distillation*, 2nd ed.; John Wiley & Sons, Inc.: Hoboken (New Jersey), 2021; DOI: 10.1002/9781119414674.

(48) Dortmund Data Bank. www.ddbst.com, 2021.

(49) Poggetto, G. D.; Castañar, L.; Adams, R. W.; Morris, G. A.; Nilsson, M. Relaxation-encoded NMR Experiments for Mixture Analysis: REST and Beer. *Chemical Communications* **2017**, *53*, 7461–7464, DOI: 10.1039/c7cc03150e.

(50) Specht, T.; Münnemann, K.; Hasse, H.; Jirasek, F. Automated Methods for Identification and Quantification of Structural Groups from Nuclear Magnetic Resonance Spectra Using Support Vector Classification. *Journal of Chemical Information and Modeling* **2021**, *61*, 143–155, DOI: 10.1021/acs.jcim.0c01186.

For Table of Contents Use Only

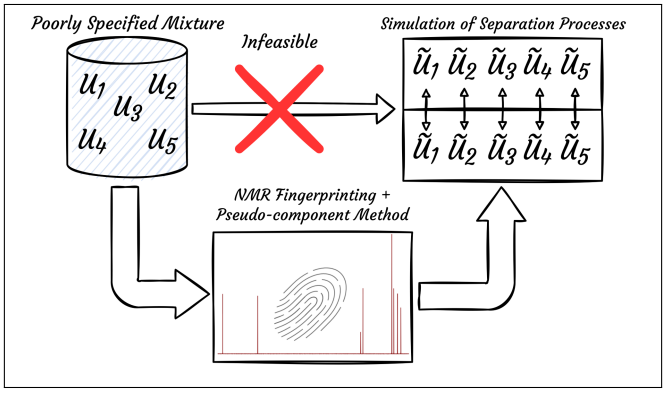

Predictive Thermodynamic Modeling of Poorly Specified Mixtures and Applications in Conceptual Fluid Separation Process Design

Thomas Specht, Hans Hasse, Fabian Jirasek*